

Effective Reduction of Nonspecific Binding by Surface Engineering of Quantum Dots with Bovine Serum Albumin for Cell-Targeted Imaging

Bingbo Zhang,^{*,†} Xiaohui Wang,[‡] Fengjun Liu,[‡] Yingsheng Cheng,[‡] and Donglu Shi^{*,†,§}

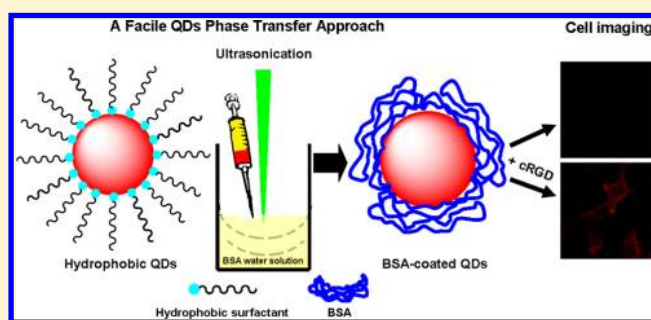
[†]The Institute for Biomedical Engineering & Nano Science, Tongji University School of Medicine, Shanghai, 200092, P. R. China

[‡]Medical Imaging Center, the Tenth People's Hospital, Tongji University, Shanghai 200072, P. R. China

[§]School of Electronic and Computing Systems, University of Cincinnati, Cincinnati, Ohio 45221, United States

Supporting Information

ABSTRACT: Quantum dots (QDs) have been widely used as fluorescent probes in cell-targeted imaging. However, nonspecific binding to cellular membranes has been a major challenge. In this study, a new approach is developed for effective reduction of nonspecific binding by bovine serum albumin (BSA)-coated QDs in cell targeting. The experimental results show efficient transfer of hydrophobic QDs from organic to aqueous phase in the presence of BSA aqueous solution under ultrasonication. This ultrasonication-based approach is facile, rapid, and efficient. Stabilization of QDs is mainly achieved by multiple mercapto groups in BSA macromolecules as multidentate ligands and partially by hydrophobic interaction between BSA and pending fatty ligands on QDs. The water solubility of QDs is enhanced by the surface amino and carboxyl groups, which also provide reaction sites for conjugation of targeting ligands. The BSA-coated QDs, with an overwhelming majority of hydrodynamic diameter size of ca. 18 nm, are colloidally stable under both acidic and basic conditions and found to exhibit strong fluorescent intensities. The nonspecific cellular binding is effectively reduced by BSA-coated QDs, compared with the mercaptopropionic acid (MPA)-coated CdTe QDs. BSA-coated QDs are further functionalized with cyclic Arg-Gly-Asp (cRGD) peptide. The cell assays indicate their high target-selectivity in integrin $\alpha_v\beta_3$ -expressed cell imaging.



INTRODUCTION

Quantum dots (QDs) are known for their monochromatic emissions, tunable wavelength, broad absorption cross section, large molar extinction coefficients, high quantum yields (QYs), and excellent photostability.^{1–3} For these unique properties, QDs have been widely used in biomedical labeling, molecule tracking, and imaging.^{4–8} However, some critical issues still remain to be addressed on their colloidal properties such as water solubility, hydrodynamic size, and colloidal stability.^{9,10} Nonspecific binding is a major challenge in biodetection.^{11,12} QDs generally attach onto the cell membranes, proteins, and other matrix materials nonspecifically, resulting in a high level of background fluorescence that degrades the signal-to-noise ratio and limits detection sensitivity. False positives are likely as a result of nonspecific binding.

Different ways have been developed to address the issue in recent years. Nie et al. reported hydroxyl (–OH)-coated QDs for minimizing nonspecific cellular binding.¹¹ Their experimental results indicated that the hydroxyl-coated QDs showed significantly reduced nonspecific binding compared to those functionalized with carboxylate, streptavidin, and poly(ethylene glycol). Further study implied that nonspecific binding was mainly associated with the surface conditions of the nano-

particles such as chemical groups, surface charge, and molecular weight of surface ligands. Therefore, generating hydroxyl groups from negatively charged carboxyl groups has become a main approach for achieving lower surface charges. PEG, known for its hydrophilia and biocompatibility, is often linked to the surfaces of nanoparticles for reduction of nonspecific binding and improving water solubilization.^{12–14} These previous studies showed that pegylated QDs with nearly neutral surface charges had significantly reduced nonspecific binding.^{12–17} Unfortunately, although achieving amazing development, these modification processes are generally tedious, high cost, and environmentally unfriendly, spoiling their advantages in biomedical applications.

BSA is an extensively used and commercially available biomacromolecule in biological applications, for its capability of reducing nonspecific binding in immunoassay.^{18,19} In this study, a facile water solubilization approach was developed based on BSA surface engineering, aiming at reducing nonspecific binding with fine nanoparticle sizes. BSA is an important

Received: July 9, 2012

Revised: October 30, 2012

Published: November 12, 2012

blood protein containing one single cysteine and eight pairs of disulfide bonds.^{20,21} These sulfhydryl compounds acting as multidentate ligands can replace the original hydrophobic ligands of QDs. Ligand exchange with multidentate compounds has become a promising trend in improving water-solubilization of hydrophobic nanoparticles, since they exhibit much stronger interactions with QD surfaces compared with that of single or dithiol ligands.^{22–25} Dihydrolipoic acid (DHLLA) ligands can enable stable interactions with QD surfaces due to the bidentate chelate effect afforded by the dithiol groups.²⁶ However, aggregation and nonspecific binding were observed, when these QDs were mixed with cationic polymer or nanoparticles in acidic solutions.²⁷ These behaviors are associated with the loss of water compatibility once the carboxylic acid end groups on the DHLLA-coated QDs are no longer ionized in the acidic solution.

Furthermore, as a zwitterionic polymer, the colloidal stability of QDs can be enhanced well by BSA coating, due to the surface amino and carboxyl groups, in both acidic and basic environments. The surface charges of QDs are also well-balanced for reduction of nonspecific binding. The phase transfer of QDs is induced by ultrasonication. This process is facile, reproducible, and rapid within 5 min. The BSA-coated QDs developed in this study have been found to exhibit good colloidal stability, high quantum yields, and pronounced reduction of nonspecific binding. Upon conjugation with cRGD peptide,^{28–30} they are highly selective for targeted integrin $\alpha_v\beta_3$ -expressed cell imaging.

EXPERIMENTAL SECTION

Materials. All reagents used were analytical grade and available commercially. These include the following: selenium powder (100 mesh, 99.99%, Aldrich), cadmium oxide (CdO, 99.5%, Aldrich), zinc oxide (ZnO, 99.9%, Sigma), sulfur (99.98%, Aldrich), tri-*n*-butylphosphine (TBP, 90%, TCI, Japan), tri-*n*-octylphosphine oxide (TOPO, 90%, Aldrich), octadecylamine (ODA, 90%, ACROS), 1-octadecene (ODE, 90%, ACROS), oleic acid (OA, 90%, Aldrich), cyclic Arg-Gly-Asp peptide (c(RGDfK), Apeptide, Shanghai), BSA (Beijing Dingguo Biotechnology Co. Ltd.), thioctic acid (99%, Sigma), and 1-ethyl-3-(3-dimethylaminopropyl)carbodiimide hydrochloride (EDC-HCl, GL Biochem (Shanghai) Ltd.). Acetone, chloroform, ethanol, dichloromethane, and argon (oxygen-free) were obtained from local suppliers. All chemicals were used without further purification. Deionized water (18.2 M Ω -cm resistivity at 25 °C) was used throughout the entire experiments.

Synthesis of Hydrophobic Surfactant-Capped Core/Shell QDs. Hydrophobic surfactant-capped QDs were synthesized according to previously reported protocols with minor modifications.^{31,32} CdSe core QD synthesis is described as follows. Briefly, 0.3 mmol of CdO, 0.4 mL of OA, and 4.0 mL of ODE were loaded into a 50 mL flask. The mixture was heated to 300 °C under an Ar flow, and CdO was dissolved to generate a colorless homogeneous solution. The solution was then cooled to room temperature, followed by adding 2.50 g of ODA and 0.50 g of TOPO into the flask. The system was heated again to 280 °C under an Ar flow. Subsequently, a selenium solution (1.8 mmol of Se powder dissolved in 2 mL of TBP) was injected quickly. Following the injection of selenium, nanocrystals were grown at 260 °C for different time periods depending on the desired sizes. The solution was found to experience color changes from colorless, to green, yellow, and finally red, which is the manifestation of QD formation. The solution was injected into chloroform. The CdSe QDs were precipitated by adding dry ethanol, collected by centrifugation, washed with methanol several times, and vacuum-dried for use.

Core/shell QDs were synthesized with the following procedures. Typically, CdSe nanocrystals dissolved in 10 mL of hexane were mixed

with 1.5 g of ODA and 5.0 g of ODE in a 25 mL three-neck flask. The flask was then switched to Ar flow to replace the air for 30 min, and then heated to 100 °C for another 5–10 min to remove hexane from the system. The reaction mixture was further heated to 240 °C for injections. The procedures of Cd, Zn, and S resource injections can be found in ref 32. The final product was diluted by hexane, followed by a methanol extraction or acetone precipitation of the nanocrystals. Excess amines were further removed by dissolving the nanocrystals in chloroform and their precipitation with acetone. In this study, CdSe/CdS^{2 ML}/Cd_{0.75}Zn_{0.25}S/Cd_{0.5}Zn_{0.5}S/Cd_{0.25}Zn_{0.75}S/ZnS^{2 ML} core/shell QDs were prepared for further experiments (ML is an acronym for monolayer). Hydrophobic surfactants capped on core/shell QDs are denoted as OA, ODA, and TOPO.

QD Phase Transfer under Ultrasonication Condition. QD/chloroform solution was transferred into a clean syringe for injection. For thorough ligand exchange, the mole ratio of BSA to QDs was kept in the range 500–1000. The weighed BSA was completely dissolved in 15 mL of deionized water in a 50 mL beaker. The beaker was placed in an ultrasonic cell crushing instrument with an ultrasonic booster (JY92-IID, Ningbo Scientz Biotechnology Co., LTD). The top of the booster was placed ca. 0.5 cm under the liquid level of BSA/water solution. The top of the long needle on the syringe was placed next to that of the booster. Ultrasonication at 300–500 W was pulsed every 10 s for a duration of 10 s. The QD/chloroform solution was slowly injected into the BSA/water solution with ultrasonication. The solution in the beaker became emulsion-like after injection, and bright homogeneous fluorescence was observed under a hand-held UV lamp. Upon injection, the sample solution was quickly stirred under reduced pressure to remove the remaining organic solvents. Finally, the BSA-coated QDs were purified by centrifugation at 100 000 g for 30 min and washing with deionized water to remove residual BSA.

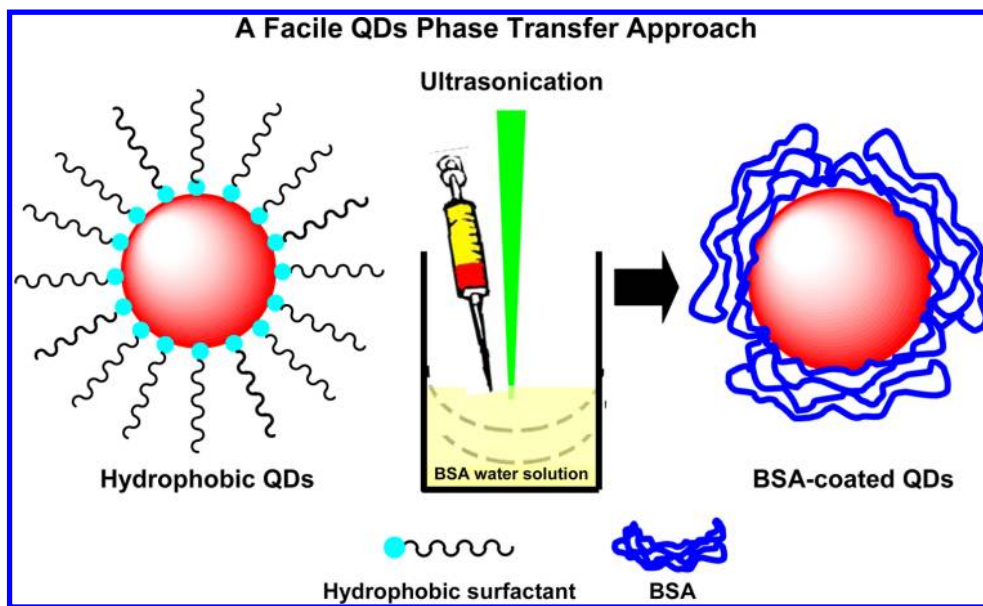
BSA-Coated QDs Functionalized with cRGD. On the basis of carbodiimide chemistry, EDC-HCl was used as the cross-linker to prepare QD-peptide bioconjugates. The BSA-coated QDs were reacted with cRGD at a QDs/cRGD/EDC-HCl molar ratio of 1:100:4000 in borate saline buffer (50 mM, pH 8.2) for 2 h at room temperature. The final bioconjugate products were purified by centrifugation at 100 000 g for 30 min and washing with 0.01 M PBS (pH 7.4) two times.

Gel Electrophoresis Analysis. BSA-coated QDs and cRGD functionalized BSA-coated QDs were prepared with a 6 \times loading buffer on a 0.7% agarose gel at 110 V in TAE buffer (1 \times) for 40 min (PowerPak Basic, Bio-Rad). The gel was illuminated with an ultraviolet trans-illuminator (Tanon Gel Image System) for fluorescence imaging of the emission bands.

Qualitative Evaluation of Nonspecific Binding with Cells. Five cell lines (HeLa, SKOV3, MCF-7, L929, and 3T3) were used in this study for evaluation of nonspecific binding by BSA-coated QDs. Cells were cultured in RPMI media with 10% fetal bovine serum (FBS) and penicillin/streptomycin (100 U/mL) at 37 °C in a humidified atmosphere containing 5% CO₂. Cells were plated in 6-well plates and cultured for 24 h. The cells were washed twice with fresh 1 \times PBS, fixed with 4% formaldehyde for 2 h, permeabilized with 0.1% Triton X for 5 min, and washed again three times with 0.01 M PBS. A 2% BSA blocking solution was added to the wells and incubated for 20 min. After the solution was aspirated, BSA- and MPA-coated CdTe QDs in the blocking solution were, respectively, added into the wells and incubated with the cells for 30 min. The cells were then washed three times with 0.01 M PBS to remove the QDs, and the cellular nucleus was stained with 4',6-diamidino-2-phenylindole (DAPI) solution (2 μ g/mL). Finally, the cells were washed three times with deionized water, and imaged under fluorescence microscopy.

Quantitative Analysis of Nonspecific Binding. HeLa and 3T3 cells were cultured in 96-well Thermo Microtiter Microplates for 24 h, fixed, and blocked with 2% BSA blocking solution. BSA- and MPA-coated CdTe QDs with concentrations ranging from 1 nM to 100 nM were loaded in the moisture chamber and incubated for 30 min at 37 °C. After washing the plates three times with 0.01 M PBS containing 0.02% Tween-20, each was measured on a Thermo Fluoroskan Ascent FL plate reader (excitation at 355 nm, emission at 620 nm).

Scheme 1. Schematic Diagram Showing the Formation of BSA-Coated QDs under Ultrasonication Condition in a One-Pot Facile Approach



Cell-Targeted Imaging. For comparison, U87 MG (integrin $\alpha_v\beta_3$ overexpressed) and MCF-7 (integrin $\alpha_v\beta_3$ low expressed) cells were used in this study. Preseed 0.2×10^5 U87 MG cells in each glass-bottomed microwell dish were incubated overnight. Parallel experiments using integrin $\alpha_v\beta_3$ -negative MCF-7 cells were carried out as a control. The cell culture medium was aspirated from the dish and the cells were washed three times with 0.01 M PBS (3–5 min each). A 2% BSA blocking solution was added and incubated for 20 min. After the solution was aspirated, BSA-coated or cRGD-functionalized BSA-coated QDs in the blocking solution were added and incubated with the cells for 30 min. The cells were then washed three times with 1× PBS to remove the QDs. Finally, the cells were imaged under fluorescence microscopy.

Characterization. Transmission Electron Microscopy (TEM). The BSA-coated QDs were dispersed in deionized water and dried onto carbon-coated copper grids before examination. TEM images were obtained with a Philips Tecnai G² F20 TEM operating at an acceleration voltage of 200 kV.

Spectrum Characterizations. The absorbance and emission spectra of hydrophobic QDs in chloroform and BSA-coated QDs in deionized water were measured on a Cary 50 spectrophotometer (Varian) and a F-4500 spectrophotometer (Hitachi), respectively.

The dispersion property of BSA-coated QDs in deionized water was measured using a particle size analyzer (Nano ZS, Malvern). The fluorescence QYs of the QDs in deionized water were measured using Rhodamine 6G as fluorescence standard.³³

RESULTS AND DISCUSSION

Phase Transfer of QDs. The schematic illustration of the one-pot facile QD phase-transfer process is shown in Scheme 1. The phase transfer is accomplished by ultrasonication. QD/chloroform solution is slowly injected into the BSA/water solution during ultrasonication. BSA as a natural biomacromolecule has one free sulfhydryl and eight pairs of disulfide bonds. Although sulfhydryl and disulfide bonds can replace the hydrophobic surfactants and bind onto the surfaces of QDs, they are inside the BSA macromolecules, resulting in impeditive contacts with QDs. This steric obstruction can be reduced by ultrasonication. Under the external physical force, the BSA macromolecules are stretched and the sulfhydryl and disulfide bonds are exposed to QDs. Ultrasonication has been found to

be a precondition for phase transfer of QDs. Once all the sulfhydryl and disulfide bonds bind onto the surfaces of QDs, the multidentate interaction is much stronger than that of the single or dithiol ligands.

DHLA is a commonly used dithiol chemical in the phase transfer of QDs.²⁶ Currently, dithiol derivatives based on DHLA have been commonly used for enhancement of colloidal stability of modified QDs.²⁷ In this study, commercially available BSA protein was selected for coating of QDs instead of chemical synthesis of multithiol compounds for low cost and time savings.

The successful phase transfer of QDs from organically soluble to water-soluble was achieved in this study. Instead of chloroform, the as-prepared QDs can only be solubilized in aqueous solution. Subsequent TEM analysis further confirms that a large proportion of the BSA-coated QDs are well-dispersed on the copper mesh after drying from water (Figure 1a) except some aggregated clusters (see Figure S1). As shown

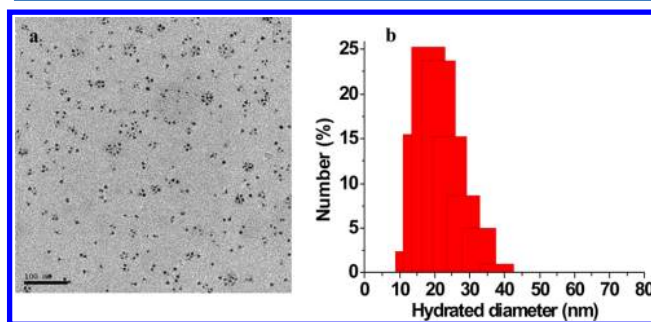


Figure 1. TEM image (a) and DLS (b) of the BSA-coated QDs.

in Figure 1b, the hydrodynamic size of BSA-coated QDs is slightly larger than that observed from TEM. This is due to BSA macromolecules being capped on QDs. The original QD core used in this study is about 8.0 nm in size, and BSA molecule is about 5.0 nm in water. Thus, the hydrodynamic diameter of BSA-coated QDs is about 18.0 nm ($8.0 + 2 \times 5.0$), which coincides with the DLS analysis. The presence of large-

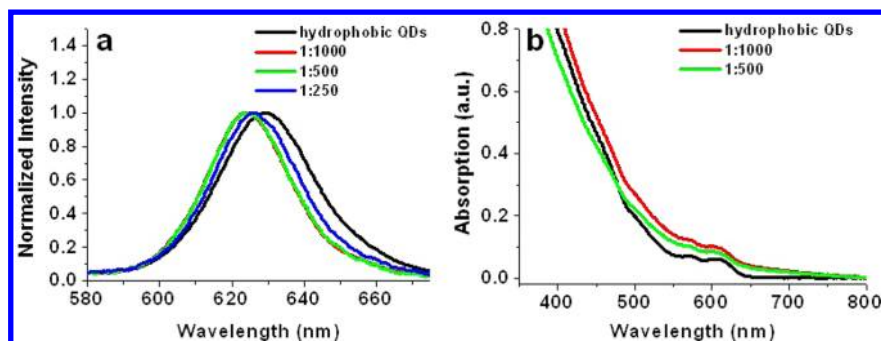


Figure 2. Photoluminescence spectra (a) and UV-vis absorption spectra (b) of BSA-coated QDs prepared with different QDs/BSA mole ratios.

sized fractions of BSA-coated QDs shown in TEM and DLS will be discussed below.

The degree of ligand exchange (phase transfer efficiency) was preliminarily evaluated by spectrum characterization. The change of QDs local surface microenvironment arising from ligand exchange can cause spectrum fluctuations.³⁴ Figure 2a shows the photoluminescence spectra of the as-prepared samples with different BSA/QD mole ratios. Consistent but respectable blue shifts (ca. 5 nm) are observed for samples of higher BSA/QD mole ratios of 500 and 1000, respectively. A smaller blue shift (ca. 3 nm) is observed at the mole ratio of 250. No further blue shift is observed for BSA/QD mole ratios greater than 500. The effect of phase transfer on absorption spectra is less pronounced as shown in Figure 2b. The as-prepared samples with BSA/QD mole ratios below 250 aggregate easily (see Figure S2). One possible explanation for this aggregation is that the hydrophobic surfactants are not efficiently replaced by limited BSA macromolecules at low BSA/QD mole ratios. The fluorescence QYs of the original hydrophobic QDs in chloroform and the BSA-coated QDs (with 500 of BSA/QDs mole ratio) in deionized water are 45% and 35%, respectively.

In order to conjugate sulfhydryl and disulfide moieties on BSA accessible for covalent binding to QD surfaces, BSA was denatured by adding sodium borohydride, and the surface ligand exchange experimental results show similar capability of the reduced BSA in the phase transfer of QDs. To simplify the chemical procedures, intact BSA was used in this study.

Mechanism of Phase Transfer. To identify the phase transfer mechanism, hydrophobic magnetic nanoparticles, OA-coated QDs, and 1-dodecanethiol (DDT)-coated CuInS₂/ZnS QDs were synthesized, respectively, in this study. The same approach was found to apply well on phase transfer of the hydrophobic magnetic nanoparticles. The only difference is the clustering of the magnetic nanoparticles (see Figure S3). Quite similar phase transfer behaviors were found between the OA-coated and the OA/ODA/TOPO-coated QDs. DDT, as the capping agent for CuInS₂/ZnS QDs, has one free thiol group, which binds on the surface of CuInS₂/ZnS QDs. This binding force is stronger than that of OA, ODA, and TOPO with QDs, which gives rise to inefficient ligand exchange by BSA. Although some CuInS₂/ZnS nanoparticles are efficiently coated by BSA (see Figure S4), a large fraction of the modified CuInS₂/ZnS QDs is found to aggregate after storage for a period of time (see Figure S2).

Fatty ligands are originally capped on the surfaces of QDs and magnetic nanoparticles. However, the results of water solubilization are found to be drastically different between BSA-coated QDs and magnetic nanoparticles under ultrasonication.

The QDs treated by BSA are individually dispersed in water solution (ca. 18 nm of hydraulics diameter, except a tiny fraction of aggregated clusters; see Figure S1), while magnetic nanoparticles (also treated by BSA) are nanoparticle clusters formed by tens of single magnetic nanoparticles (ca. 90 nm of hydraulics diameter, Figure S3). These results indicate higher affinity of BSA macromolecules on the surface of QDs than on the magnetic nanoparticles. It should be noted that the physicochemical properties of surface capping ligands on QDs and magnetic nanoparticles are nearly the same. Thus, a hypothesis is put forward that BSA macromolecules could replace the original organic ligands on the surface of QDs, but not on the magnetic nanoparticles. This difference is understood by higher affinity between the -SH, -S-S- groups, and Cd/Zn, when compared with the Fe atoms.

The chemical -SH group has been extensively reported as an excellent affinitive ligand for aqueous QDs synthesis³⁵ and on ligand exchange of hydrophobic QDs.^{22–25,36,37} However, there have been few reports on the possibility of -S-S- groups being responsible for original organic ligand exchange on the surface of QDs. In this study, the following experiment was conducted to address this issue. Thiocetic acid was used as a disulfide compound model for phase transfer of QDs according to the procedures described in this study. Interestingly, hydrophobic QDs were found to transfer successfully into the water phase under ultrasonication, while phase transfer cannot be achieved under magnetic stirring (see Figure S5). The -S-S- bonds cannot be reduced to -SH by ultrasonication, which is confirmed with an Ellman's Test Kit. It is noted that all the observed results in this study present both BSA and ultrasonication as necessary for QD phase transfer. A hypothesis is consequently put forward that radical formation (-S[•]) occurs transiently during sonication, but the -S-S- bridge reforms afterward. We are considering verifying this hypothesis with experimental evidence. However, the thiocetic acid modified QD precipitate appeared after one day storage, which indicates that thiocetic acid modified QDs are not stable. In terms of BSA, it has one free mercapto group and eight pairs of disulfide bonds. These sulfhydryl compounds, acting as multidentate ligands, have high affinity for Cd/Zn atoms. BSA is quite a bit larger than thiocetic acid in molecular structure, suggesting it has multidentate sites for conjugation with QDs. Thus, these render good colloidal stability of BSA-coated QDs (Figure 3). Although ligand exchange is executed under ultrasonication conditions, a tiny fraction of aggregates remains (Figure S1), and these aggregates are also shown in the DLS data. This aggregation could be attributed to insufficient ligand exchange and subsequent hydrophobic interactions between BSA and the pendant fatty acid chains on the surface of QDs.

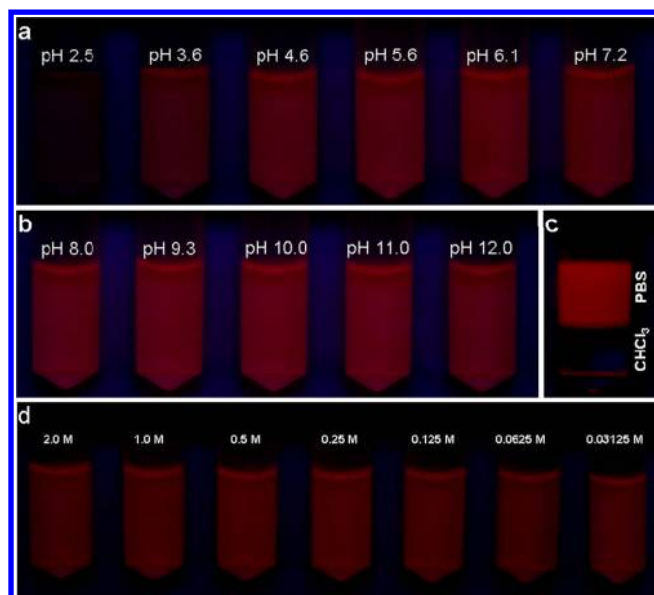


Figure 3. Luminescent images (a,b) of the BSA-coated QD emissions at various pH buffer solutions (pH varies from 2.5 to 12.0 after 7 days at room temperature), phase transfer image of the as-prepared BSA-coated QDs, excited with a hand-held UV lamp at 365 nm (c), and luminescent images (d) of the BSA-coated QD emission in sodium chloride water solutions with various ionic strengths after 7 days at room temperature. The BSA-coated QDs were prepared with 500 mole ratio of BSA/QDs.

The aggregated QDs are smaller than 50 nm, and also have quite good colloidal stability.

For Fe_3O_4 magnetic nanoparticles, however, the original organic ligands are hardly replaced by BSA macromolecules due to weak interactions between -SH-/S-S- bonds and Fe atoms. Fe_3O_4 nanoparticles can be made water-soluble via hydrophobic interactions with BSA macromolecules. BSA has been reported to exhibit high affinity with fatty acids, hematin, and bilirubin. It is also known for a broad affinity with small, negatively charged aromatic compounds via a combination of hydrophobic and electrostatic interactions.^{38,39} The hydrophobic fatty acids, coated on the Fe_3O_4 magnetic nanoparticles, can also bond with BSA proteins. This bonding evolves into clustering of magnetic nanoparticles under ultrasonication in

the presence of the BSA/water phase. The clustering process is also facile, reproducible, and rapid.

Stability Study of BSA-Coated QDs. Figure 3 shows the colloidal stability of the BSA-coated QDs at various pH values and ionic strengths. As expected, the BSA-coated QDs are stable over a wide range of pH values (pH 2.5–12) showing no signs of sedimentation. This indicates the dependence of the BSA-coated QDs on electrostatic stabilization from the amino and carboxyl groups. As is well-known, the BSA macromolecules can be ionized in both acidic and alkaline solutions. The large quantity of amino and carboxyl groups on BSA macromolecules renders BSA with effective buffering capacity that posts significant resistance to harsh chemical environments.

Figure 4 shows the effects of pH values and ionic strengths on the photoluminescence of BSA-coated QDs. Overall, the emission intensity of the BSA-coated QDs increases with increasing pH value. QDs in acid solution exhibit slight erosion,⁴⁰ that is detrimental to the local surface environment of the QDs, leading to reduced fluorescence intensity. The decrease of photoluminescence at pH 5.6 and 6.1 is observed, respectively, attributable to the isoelectric point of BSA in this pH range.⁴¹ The structure of BSA is found to change at these pH values, responsible for variations of fluorescence. Little or no change in photoluminescence intensity is observed at various ionic strengths (see Figure 4b). These experimental results indicate good stability of QDs, capped with the multidentate BSA in high ionic strength conditions. Moreover, these results are directly applicable to intracellular and in vivo studies, where the ionic concentration is known to be high.

Nonspecific Cellular Binding of BSA-Coated QDs. BSA is frequently used as a nonspecific binding blocking agent. BSA macromolecules can be absorbed onto the interspaces of ligands on the surface of nanoparticles. In this way, the nanoparticles are blocked by BSA to lower nonspecific binding when labeled with targeting ligands, such as antibodies, peptides, and other proteins. In this study, BSA as multidentate ligands is used to exchange the original organic ligands on the surface of QDs to reduce nonspecific cellular binding. The role of the BSA is twofold: one as the ligand-exchange agent for water-solubilization of QDs, and the other for reduction of nonspecific cellular binding.

Nonspecific cellular binding was both qualitatively and quantitatively evaluated by fluorescent microscopy and

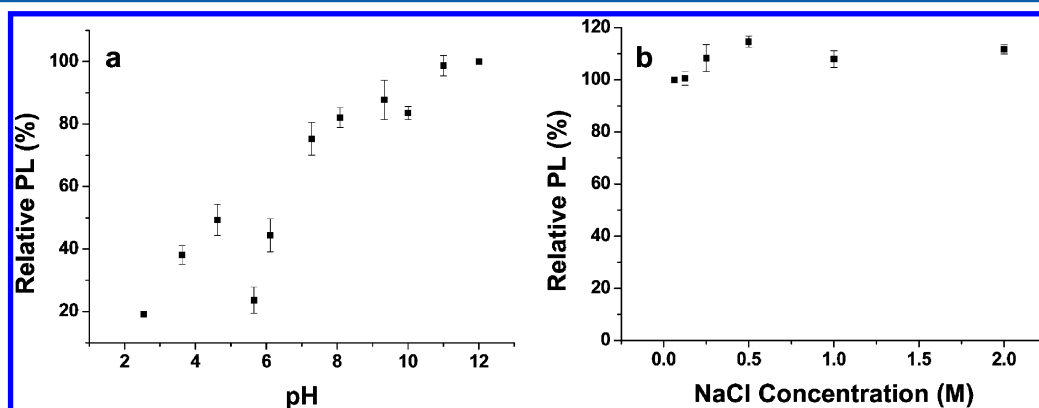


Figure 4. Effects of pH values (a) and ionic strengths (b) on the photoluminescence of BSA-coated QDs, prepared with 500 mole ratio of BSA/QDs. The resulting photoluminescence spectra are background-corrected, integrated, and normalized. The photoluminescence emissions from QDs with pH 12.0 (a) and the lowest ionic strength (b) are set to 100%.

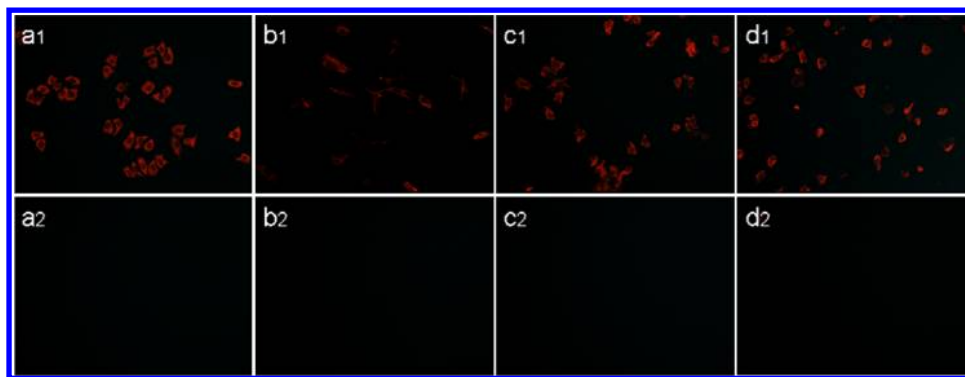


Figure 5. Fluorescence microscopy images of the MPA-coated CdTe QDs (a1 to d1) as a reference and the BSA-coated QDs (a2 to d2) nonspecifically bonded to fixed cells. Cells were cultured by QDs at 50 nM concentrations, and then washed. The nonspecific cellular binding was done in four different cell lines: HeLa (a), SKOV3 (b), MCF-7 (c), and L929 (d).

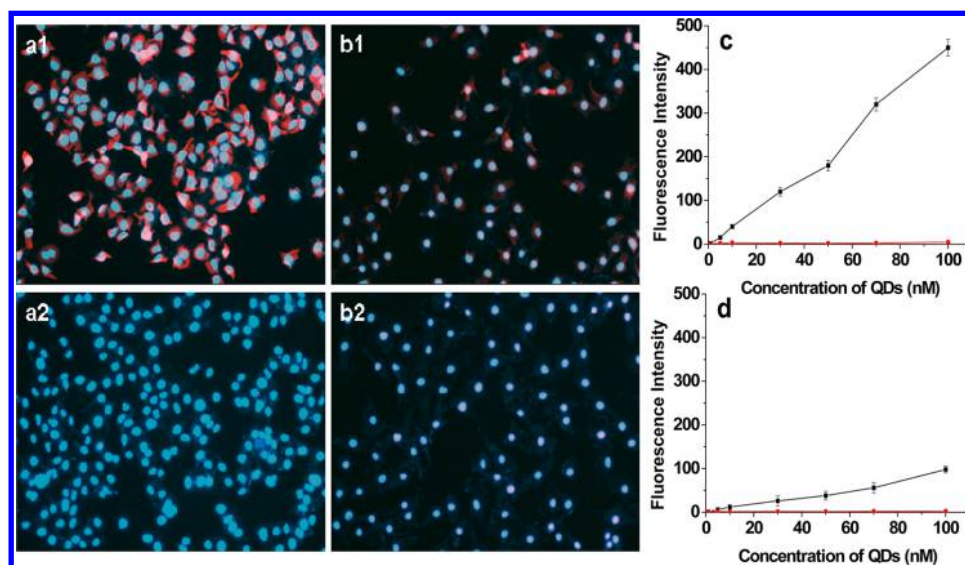


Figure 6. Fluorescent imaging comparison (a and b) and quantitative evaluation (c and d) of nonspecific cellular binding of MPA-coated CdTe QDs (a1, b1, ■) and BSA-coated QDs (a2, b2, ●) on HeLa (a) and 3T3 (b) cells.

fluorescence measurement plate reader of cell cultures grown on 96-well plates. Figures 5 and 6 show significant amounts of nonspecific cellular binding of MPA-coated QDs on all selected cell lines, while no obvious nonspecific cellular binding is found for BSA-coated QDs. Although BSA used for cell blocking can adsorb on MPA-coated QDs for reduction of its nonspecific binding with the involved cells, the resulting nonspecific signals are much higher than that of BSA-coated QDs. This suggests that the BSA adsorption on MPA-coated QDs is less efficient than ultrasonication, which could explain the difference observed between BSA-coated QDs and MPA-coated QDs on nonspecific cellular binding. For further comparison of the performance of BSA-coated and MPA-coated QDs on nonspecific cellular binding, cell experiments have been performed in the absence of serum protein blocking (Figure S6). It also shows that BSA-coated QDs have superior performance on reduction of nonspecific cellular binding.

BSA are known for nonspecific binding reduction, and are widely used in biological detection.^{42,43} As indicated by these results, BSA macromolecules as multidentate ligands are well-coated on the surface of QDs, showing excellent reduction of nonspecific cellular binding. Interestingly, the degree of nonspecific cellular binding of MPA-coated CdTe QDs on HeLa cells is higher than that on 3T3 cells. This is consistent

with a previous report.¹² Rosenthal et al. found the degrees of nonspecific binding of QDs to be dependent on cell types. In their study, nonspecific binding of QDs on 3T3 cells was found to be much lower than that on other cell types.

Nonspecific cellular binding of QDs is a complex issue. It can be attributed to hydrophobic interactions between the ligands of QDs and lipids on the cell membranes. It is also associated with the electrostatic interactions between the cells and the negatively charged groups on the surfaces of QDs.^{11,12,44} Different cell types express a variety of proteins or lipids on their surfaces that allow for interactions with exposed hydrophobic regions of QDs. Thus, the complete coating of QDs is critical to nonspecific cellular binding. In this study, hydrophobic surfactants on the surfaces of QDs are mainly exchanged as a result of multidentate BSA ligands, as evidenced in the cellular binding experiments.

Nonspecific cellular binding by electrostatic interaction was studied in a previous study.¹¹ Nonspecific cellular binding was remarkably reduced by hydroxylation of carboxylated QDs. Hydroxylation reduces surface charges of QDs, thus weakening the electrostatic interactions between QDs and cell membranes. The surface charge is directly dependent on the chemical groups of QDs. MPA-coated QDs have abundant carboxyl groups, contributing to high negative surface potentials. The

amino and carboxyl groups on QDs surfaces, which are oppositely charged, give rise to partial neutralization of surface potentials. This is clarified in Table 1, showing that, in the same buffer, BSA-coated QDs hold lower zeta potential (-19.5 mV) than MPA-coated QDs (-28.8 mV).

Table 1. Properties of the BSA-Coated QDs and MPA-Coated QDs Used in This Study

QDs	hydrodynamic diameter (nm)	zeta potential (mV)	buffer
BSA-coated QDs	18.0	-19.5	borate saline buffer (50 mM, pH8.2).
MPA-coated QDs	6.0	-28.8	borate saline buffer (50 mM, pH8.2).

The effective reduction of nonspecific cellular binding is also observed on fluorescent BSA-coated gold (Au) nanoclusters (Au NCs) (see Figure S7 and S8). The Au NCs were prepared via biomineralization by using BSA as a scaffold.⁴⁵ The fluorescent Au NCs are capped by BSA. Due to combined effects of surface coating and partial neutralization, the BSA-coated QDs and Au NCs are particularly effective in reducing nonspecific cellular binding.

Targeted Cellular Imaging of BSA-Coated QDs. BSA-coated QDs with significantly reduced nonspecific cellular binding have valuable applications in biomedical detection, particularly in cell-targeted imaging. In this study, targeted cellular imaging using BSA-coated QDs was carried out by functionalization with cRGD peptide. The successful conjugation was demonstrated by agarose gel electrophoresis (see Figure S9). Under excitation, there are two distinguishable narrow and bright bands, due to the difference in electrophoresis characteristics between cRGD-functionalized and unfunctionalized BSA-coated QDs. The remarkably narrow bands suggest that the BSA-coated QDs have quite homogeneous distributions of sizes and charges.⁴⁶ The peptide of cRGD has a high binding affinity with integrin $\alpha_v\beta_3$, and it is extensively used as the targeting ligand for integrin $\alpha_v\beta_3$ expressed cells or vascularization imaging.^{47–51}

Figure 7 shows cRGD-functionalized BSA-coated QDs having different binding affinities between MCF-7 and U87 MG cells. U87 MG cells overexpress integrin $\alpha_v\beta_3$, while MCF-7 cells exhibit low expressions.⁵² As a result, many more QDs

are captured by U87 MG cells. Unfunctionalized BSA-coated QDs exhibit insignificant binding to U87 MG cells. These results indicate little or no nonspecific cellular binding of the BSA-coated QDs to U87 MG cells. Otherwise, the QD emission on cells is not distinguishable between nonspecific binding and specific targeting. These cellular specific imaging data indicate excellent reduction of nonspecific binding by BSA-coated QDs.

The cytotoxicity test was conducted for the BSA-coated QDs on normal L929 cells. No significant cytotoxicity was found at the concentrations indicated (Figure S10).

CONCLUSIONS

In conclusion, we have developed a facile QD phase transfer approach by surface engineering of QDs with BSA macromolecules under ultrasonication conditions for reduction of nonspecific cellular binding and cell-targeted imaging. The BSA-functionalized QDs exhibit excellent colloidal stability with fine hydrodynamic size distribution in a wide range of pH and ionic strength values. In particular, the BSA-coated QDs are experimentally shown to be effective in the reduction of nonspecific cellular binding. Furthermore, BSA-coated QDs are labeled with cRGD peptides for targeted integrin $\alpha_v\beta_3$ imaging. The advantages of BSA-coated QDs include straightforward synthesis, high colloidal stability, and significantly reduced nonspecific binding. These are therefore proved to be ideal nano systems for biomedical labeling, targeting, and imaging.

ASSOCIATED CONTENT

Supporting Information

Synthesis procedures of MPA-coated CdTe QDs, oleic acid capped QDs, hydrophobic iron oxide magnetic nanoparticles, CuInS₂/ZnS QDs, and AuNCs; TEM of BSA modified QDs, iron oxide, and CuInS₂/ZnS nanoparticles under ultrasonication condition; colloidal stability study of BSA-coated different surfactant-capped QDs after storage; digital image of the thioctic acid-coated QDs by ultrasonication; spectral characteristic and nonspecific cellular binding of AuNCs; gel electrophoresis analysis of the cRGD conjugation to BSA-coated QDs; MTT protocol and MTT data. This material is available free of charge via the Internet at <http://pubs.acs.org>.

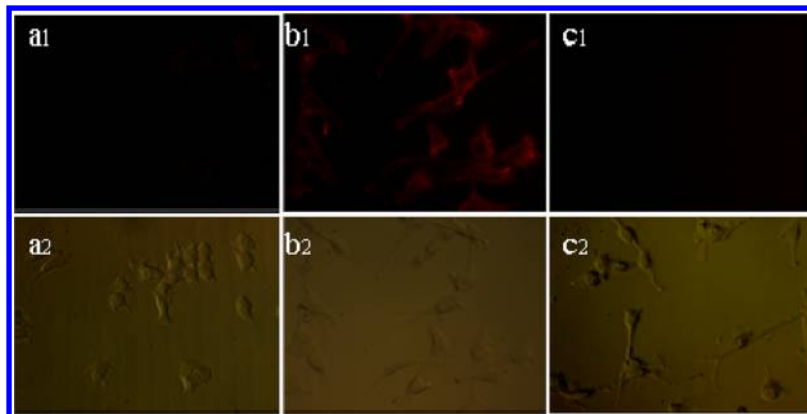


Figure 7. Staining of fixed human breast cancer MCF-7 cells (a, integrin $\alpha_v\beta_3$ -negative) and human glioblastoma U87 MG cells (b, integrin $\alpha_v\beta_3$ -positive) using 5 nM of cRGD-functionalized BSA-coated QDs. Staining of U87 MG cells with 5 nM of BSA-coated QDs is also shown in (c). Images (a1 to c1) are fluorescent pictures, and (a2 to c2) are their corresponding bright-field counterparts.

■ AUTHOR INFORMATION

Corresponding Author

*E-mail: bingbozhang@tongji.edu.cn (Bingbo Zhang); donglu.shi@uc.edu (Donglu Shi). Tel: (+) 86-21-65983706-819. Fax: (+) 86-21-65983706-0.

Notes

The authors declare no competing financial interest.

■ ACKNOWLEDGMENTS

This work was supported by the National Natural Science Foundation of China (51003078, 81171393, 81271629); the Nanotechnology Program of Shanghai Science & Technology Committee (11 nm0504500); the Program for Young Excellent Talents in Tongji University (2009KJ072), and the Fundamental Research Funds for the Central Universities.

■ REFERENCES

- (1) Resch-Genger, U.; Grabolle, M.; Cavaliere-Jaricot, S.; Nitschke, R.; Nann, T. Quantum dots versus organic dyes as fluorescent labels. *Nat. Methods* **2008**, *5* (9), 763–775.
- (2) Chan, W. C.; Nie, S. Quantum dot bioconjugates for ultrasensitive nonisotopic detection. *Science* **1998**, *281* (5385), 2016–8.
- (3) Alivisatos, A. P.; Gu, W. W.; Larabell, C. Quantum dots as cellular probes. *Annu. Rev. Biomed. Eng.* **2005**, *7*, 55–76.
- (4) Medintz, I. L.; Uyeda, H. T.; Goldman, E. R.; Mattoussi, H. Quantum dot bioconjugates for imaging, labelling and sensing. *Nat. Mater.* **2005**, *4* (6), 435–46.
- (5) Michalet, X.; Pinaud, F. F.; Bentolila, L. A.; Tsay, J. M.; Doose, S.; Li, J. J.; Sundaresan, G.; Wu, A. M.; Gambhir, S. S.; Weiss, S. Quantum dots for live cells, in vivo imaging, and diagnostics. *Science* **2005**, *307* (5709), 538–544.
- (6) Silva, G. A. Quantum dot nanotechnologies for neuroimaging. *Nanoneuroscience and Nanoneuropharmacology* **2009**, *180*, 19–34.
- (7) Yukawa, H.; Kagami, Y.; Watanabe, M.; Oishi, K.; Miyamoto, Y.; Okamoto, Y.; Tokeshi, M.; Kaji, N.; Noguchi, H.; Ono, K.; Sawada, M.; Baba, Y.; Hamajima, N.; Hayashi, S. Quantum dots labeling using octa-arginine peptides for imaging of adipose tissue-derived stem cells. *Biomaterials* **2010**, *31* (14), 4094–4103.
- (8) Klostranec, J. M.; Chan, W. C. W. Quantum dots in biological and biomedical research: Recent progress and present challenges. *Adv. Mater.* **2006**, *18* (15), 1953–1964.
- (9) Liu, W. H.; Greytak, A. B.; Lee, J.; Wong, C. R.; Park, J.; Marshall, L. F.; Jiang, W.; Curtin, P. N.; Ting, A. Y.; Nocera, D. G.; Fukumura, D.; Jain, R. K.; Bawendi, M. G. Compact Biocompatible Quantum Dots via RAFT-Mediated Synthesis of Imidazole-Based Random Copolymer Ligand. *J. Am. Chem. Soc.* **2010**, *132* (2), 472–483.
- (10) Zhang, B. B.; Xing, D.; Lin, C.; Guo, F. F.; Zhao, P.; Wen, X. J.; Bao, Z. H.; Shi, D. L. Improving colloidal properties of quantum dots with combined silica and polymer coatings for in vitro immunofluorescence assay. *J. Nanopart. Res.* **2011**, *13* (6), 2407–2415.
- (11) Kairdolf, B. A.; Mancini, M. C.; Smith, A. M.; Nie, S. M. Minimizing nonspecific cellular binding of quantum dots with hydroxyl-derivatized surface coatings. *Anal. Chem.* **2008**, *80* (8), 3029–3034.
- (12) Bentzen, E. L.; Tomlinson, I. D.; Mason, J.; Gresch, P.; Warnement, M. R.; Wright, D.; Sanders-Bush, E.; Blakely, R.; Rosenthal, S. J. Surface modification to reduce nonspecific binding of quantum dots in live cell assays. *Bioconjugate Chem.* **2005**, *16* (6), 1488–1494.
- (13) Simpson, C. A.; Agrawal, A. C.; Balinski, A.; Harkness, K. M.; Cliffl, D. E.; Short-Chain, P. E. G. Mixed Monolayer Protected Gold Clusters Increase Clearance and Red Blood Cell Counts. *ACS Nano* **2011**, *5* (5), 3577–3584.
- (14) Bagwe, R. P.; Hilliard, L. R.; Tan, W. H. Surface modification of silica nanoparticles to reduce aggregation and nonspecific binding. *Langmuir* **2006**, *22* (9), 4357–4362.
- (15) Nicolas, J.; Brambilla, D.; Carion, O.; Pons, T.; Maksimovic, I.; Larquet, E.; Le Droumaguet, B.; Andrieux, K.; Dubertret, B.; Couvreur, P. Quantum dot-loaded PEGylated poly(alkyl cyanoacrylate) nanoparticles for in vitro and in vivo imaging. *Soft Matter* **2011**, *7* (13), 6187–6193.
- (16) Song, E. Q.; Zhang, Z. L.; Luo, Q. Y.; Lu, W.; Shi, Y. B.; Pang, D. W. Tumor Cell Targeting Using Folate-Conjugated Fluorescent Quantum Dots and Receptor-Mediated Endocytosis. *Clin. Chem.* **2009**, *55* (5), 955–963.
- (17) Daou, T. J.; Li, L.; Reiss, P.; Jossierand, V.; Texier, I. Effect of Poly(ethylene glycol) Length on the in Vivo Behavior of Coated Quantum Dots. *Langmuir* **2009**, *25* (5), 3040–3044.
- (18) Wakayama, J.; Sekiguchi, H.; Akanuma, S.; Ohtani, T.; Sugiyama, S. Methods for reducing nonspecific interaction in antibody-antigen assay via atomic force microscopy. *Anal. Biochem.* **2008**, *380* (1), 51–58.
- (19) Li, P.; Abolmaaty, A.; D'Amore, C.; Demming, S.; Anagnostopoulos, C.; Faghri, M. Development of an ultrafast quantitative heterogeneous immunoassay on pre-functionalized poly-(dimethylsiloxane) microfluidic chips for the next-generation immunosensors. *Microfluid. Nanofluid.* **2009**, *7* (4), S93–S98.
- (20) Carter, D. C.; Ho, J. X. Structure of Serum-Albumin. *Adv. Protein Chem.* **1994**, *45* (45), 153–203.
- (21) Peters, T., Jr. Serum albumin. *Adv. Protein Chem.* **1985**, *37*, 161–245.
- (22) Algar, W. R.; Krull, U. J. Multidentate surface ligand exchange for the immobilization of CdSe/ZnS quantum dots and surface quantum dot-oligonucleotide conjugates. *Langmuir* **2008**, *24* (10), 5514–20.
- (23) Huang, X.; Li, B.; Zhang, H.; Hussain, I.; Liang, L.; Tan, B. Facile preparation of size-controlled gold nanoparticles using versatile and end-functionalized thioether polymer ligands. *Nanoscale* **2011**, *3* (4), 1600–7.
- (24) Tang, Z.; Xu, B.; Wu, B.; Germann, M. W.; Wang, G. Synthesis and structural determination of multidentate 2,3-dithiol-stabilized Au clusters. *J. Am. Chem. Soc.* **2010**, *132* (10), 3367–74.
- (25) Cui, Y.; Gong, X. Q.; Zhu, S. J.; Li, Y. H.; Su, W. Y.; Yang, Q. H.; Chang, J. An effective modified method to prepare highly luminescent, highly stable water-soluble quantum dots and its preliminary application in immunoassay. *J. Mater. Chem.* **2012**, *22* (2), 462–469.
- (26) Mattoussi, H.; Mauro, J. M.; Goldman, E. R.; Anderson, G. P.; Sundar, V. C.; Mikulec, F. V.; Bawendi, M. G. Self-assembly of CdSe-ZnS quantum dot bioconjugates using an engineered recombinant protein. *J. Am. Chem. Soc.* **2000**, *122* (49), 12142–12150.
- (27) Uyeda, H. T.; Medintz, I. L.; Jaiswal, J. K.; Simon, S. M.; Mattoussi, H. Synthesis of compact multidentate ligands to prepare stable hydrophilic quantum dot fluorophores. *J. Am. Chem. Soc.* **2005**, *127* (11), 3870–3878.
- (28) Alves, S.; Correia, J. D.; Gano, L.; Rold, T. L.; Prasanphanich, A.; Haubner, R.; Rupprich, M.; Alberto, R.; Decristoforo, C.; Santos, I.; Smith, C. J. In vitro and in vivo evaluation of a novel 99mTc(CO)3-pyrazolyl conjugate of cyclo-(Arg-Gly-Asp-d-Tyr-Lys). *Bioconjugate Chem.* **2007**, *18* (2), 530–7.
- (29) Chen, X.; Hou, Y.; Tohme, M.; Park, R.; Khankaldyyan, V.; Gonzales-Gomez, I.; Bading, J. R.; Laug, W. E.; Conti, P. S. Pegylated Arg-Gly-Asp peptide: 64Cu labeling and PET imaging of brain tumor alphavbeta3-integrin expression. *J. Nucl. Med.* **2004**, *45* (10), 1776–83.
- (30) Hart, S. L.; Knight, A. M.; Harbottle, R. P.; Mistry, A.; Hunger, H. D.; Cutler, D. F.; Williamson, R.; Coutelle, C. Cell binding and internalization by filamentous phage displaying a cyclic Arg-Gly-Asp-containing peptide. *J. Biol. Chem.* **1994**, *269* (17), 12468–74.
- (31) Peng, Z. A.; Peng, X. G. Formation of high-quality CdTe, CdSe, and CdS nanocrystals using CdO as precursor. *J. Am. Chem. Soc.* **2001**, *123* (1), 183–184.
- (32) Li, J. J.; Wang, Y. A.; Guo, W. Z.; Keay, J. C.; Mishima, T. D.; Johnson, M. B.; Peng, X. G. Large-scale synthesis of nearly monodisperse CdSe/CdS core/shell nanocrystals using air-stable

reagents via successive ion layer adsorption and reaction. *J. Am. Chem. Soc.* **2003**, *125* (41), 12567–12575.

(33) Fischer, M.; Georges, J. Fluorescence quantum yield of rhodamine 6G in ethanol as a function of concentration using thermal lens spectrometry. *Chem. Phys. Lett.* **1996**, *260* (1–2), 115–118.

(34) Wang, W.; Liu, G. K.; Cho, H. S.; Guo, Y.; Shi, D.; Lian, J.; Ewing, R. C. Surface charge induced Stark effect on luminescence of quantum dots conjugated on functionalized carbon nanotubes. *Chem. Phys. Lett.* **2009**, *469* (1–3), 149–152.

(35) Zhang, H.; Wang, L. P.; Xiong, H. M.; Hu, L. H.; Yang, B.; Li, W. Hydrothermal synthesis for high-quality CdTe nanocrystals. *Adv. Mater.* **2003**, *15* (20), 1712–1715.

(36) Zheng, Y. G.; Yang, Z. C.; Li, Y. Q.; Ying, J. Y. From glutathione capping to a crosslinked, phytochelatin-like coating of quantum dots. *Adv. Mater.* **2008**, *20* (18), 3410–3415.

(37) Aldana, J.; Wang, Y. A.; Peng, X. Photochemical instability of CdSe nanocrystals coated by hydrophilic thiols. *J. Am. Chem. Soc.* **2001**, *123* (36), 8844–50.

(38) Goodman, D. S. The Interaction of Human Serum Albumin with Long-chain Fatty Acid Anions. *J. Am. Chem. Soc.* **1958**, *80* (5), 3892–3808.

(39) Aki, H.; Yamamoto, M. Thermodynamic characterization of drug binding to human serum albumin by isothermal titration microcalorimetry. *J. Pharm. Sci.* **1994**, *83* (12), 1712–6.

(40) Aldana, J.; Lavelle, N.; Wang, Y.; Peng, X. Size-dependent dissociation pH of thiolate ligands from cadmium chalcogenide nanocrystals. *J. Am. Chem. Soc.* **2005**, *127* (8), 2496–504.

(41) Ghitescu, L.; Desjardins, M.; Bendayan, M. Immunocytochemical study of glomerular permeability to anionic, neutral and cationic albumins. *Kidney Int* **1992**, *42* (1), 25–32.

(42) Sakai, G.; Nakata, S.; Uda, T.; Miura, N.; Yamazoe, N. Highly selective and sensitive SPR immunosensor for detection of methamphetamine. *Electrochim. Acta* **1999**, *44* (21–22), 3849–3854.

(43) Festag, G.; Steinbruck, A.; Wolff, A.; Csaki, A.; Moller, R.; Fritzsche, W. Optimization of gold nanoparticle-based DNA detection for microarrays. *Journal of Fluorescence* **2005**, *15* (2), 161–170.

(44) Mao, H.; Chen, H. W.; Wang, L. Y.; Yeh, J.; Wu, X. Y.; Cao, Z. H.; Wang, Y. A.; Zhang, M. M.; Yang, L. Reducing non-specific binding and uptake of nanoparticles and improving cell targeting with an antifouling PEO-b-P gamma MPS copolymer coating. *Biomaterials* **2010**, *31* (20), 5397–5407.

(45) Ying, J. Y.; Xie, J. P.; Zheng, Y. G. Protein-Directed Synthesis of Highly Fluorescent Gold Nanoclusters. *J. Am. Chem. Soc.* **2009**, *131* (3), 888–889.

(46) Pellegrino, T.; Manna, L.; Kudera, S.; Liedl, T.; Koktysh, D.; Rogach, A. L.; Keller, S.; Radler, J.; Natile, G.; Parak, W. J. Hydrophobic nanocrystals coated with an amphiphilic polymer shell: A general route to water soluble nanocrystals. *Nano Lett.* **2004**, *4* (4), 703–707.

(47) Li, Z. M.; Huang, P.; Zhang, X. J.; Lin, J.; Yang, S.; Liu, B.; Gao, F.; Xi, P.; Ren, Q. S.; Cui, D. X. RGD-Conjugated Dendrimer-Modified Gold Nanorods for in Vivo Tumor Targeting and Photothermal Therapy. *Mol. Pharmaceutics* **2010**, *7* (1), 94–104.

(48) Danhier, F.; Vroman, B.; Lecouturier, N.; Crockart, N.; Pourcelle, V.; Freichels, H.; Jerome, C.; Marchand-Brynaert, J.; Feron, O.; Preat, V. Targeting of tumor endothelium by RGD-grafted PLGA-nanoparticles loaded with Paclitaxel. *J. Controlled Release* **2009**, *140* (2), 166–173.

(49) Nasongkla, N.; Shuai, X.; Ai, H.; Weinberg, B. D.; Pink, J.; Boothman, D. A.; Gao, J. M. cRGD-functionalized polymer micelles for targeted doxorubicin delivery. *Angew. Chem., Int. Ed.* **2004**, *43* (46), 6323–6327.

(50) Cai, W. B.; Shin, D. W.; Chen, K.; Gheysens, O.; Cao, Q. Z.; Wang, S. X.; Gambhir, S. S.; Chen, X. Y. Peptide-labeled near-infrared quantum dots for imaging tumor vasculature in living subjects. *Nano Lett.* **2006**, *6* (4), 669–676.

(51) Gao, J. H.; Chen, K.; Xie, R. G.; Xie, J.; Yan, Y. J.; Cheng, Z.; Peng, X. G.; Chen, X. Y. In Vivo Tumor-Targeted Fluorescence

Imaging Using Near-Infrared Non-Cadmium Quantum Dots. *Bioconjugate Chem.* **2010**, *21* (4), 604–609.

(52) Cai, W. B.; Chen, X. Y. Preparation of peptide-conjugated quantum dots for tumor vasculature-targeted imaging. *Nat. Protoc.* **2008**, *3* (1), 89–96.